TABLE I. Experimental results and comparison with the Born approximation (BA) (see text). The angles given for θ_{min} in the Born approximation are the angles θ_K of the momentum transfer.

Excited state	E (eV)	θ_e (deg)	λ Expt[a]	λ BA	$\lvert\chi\rvert$ (deg) Expt[a]	$\lvert\chi\rvert$ (deg) BA	θ_{min} (deg) Expt[a]	θ_{min} (deg) BA
$3\,^1P$	77.7	30	0.45 ± 0.01	0.231	53 ± 2	0	50 ± 2	61.3
$2\,^1P$	80.0	16	0.39 ± 0.02	0.290	38 ± 2	0	53 ± 2	57.4

[a]Uncertainties quoted for λ and χ represent 1 standard deviation.

indicate significant deviations from the predictions of the Born approximation.

Work is continuing to measure the dependence of λ and χ on E and θ_e for both excited states. The results will map out in greater detail than heretofore possible the deviations of various electron-atom collision theories from experiment.

The authors are grateful to Professor R. Novick and Dr. M. Levitt for their assistance in the early stages of the experiment and to Professor P. G. Burke for helpful discussions.

*Work supported by the U. S. Air Force Office of Scientific Research under Grant No. AFOSR-68-1454, the British Science Research Council, and the University Grants Committee.

†European Science Exchange Fellow. Permanent address: U. E. R. de Physique, Universitè de Paris, Paris 7, France.

‡Frank Knox Memorial Traveling Fellow of Harvard University, 1971–1972.

[1]J. Macek and D. H. Jaecks, Phys. Rev. A 4, 2288 (1971).

[2]J. Wykes, J. Phys. B: Proc. Phys. Soc., London 5, 1126 (1972).

[3]B. L. Moiseiwitsch and S. J. Smith, Rev. Mod. Phys. 40, 238 (1968).

[4]H. Kleinpoppen, in *Physics of One- and Two-Electron Atoms*, edited by F. Bopp and H. Kleinpoppen (North-Holland, Amsterdam, 1969), pp. 612–631.

[5]It can be shown by elementary angular-momentum algebra that for the wave function ψ of Eq. (1) the expectation value of the component of atomic orbital angular momentum perpendicular to the plane of scattering is $-2[\lambda(1-\lambda)]^{1/2}\sin\chi$.

[6]The spherical polar coordinate system is centered on the intersection of the helium and electron beams with the direction of the latter defining the polar axis and the axis of quantization. Zenith and azimuth angles are measured in the usual way. The scattering plane, defined by the incident electron beam and the axis of the electron analyzer, can be described by $\varphi = 0$.

[7]R. E. Bell, in *Alpha, Beta, and Gamma Ray Spectroscopy*, edited by K. Siegbahn (North-Holland, Amsterdam, 1966), Vol. 2, pp. 905–929.

[8]R. E. Imhof and F. H. Read, J. Phys. B: Proc. Phys. Soc., London 4, 450 (1971).

Relativistic Electron Beam Heating of a Fully Ionized Plasma*

P. Korn, F. Sandel, and C. B. Wharton
Laboratory of Plasma Studies, Cornell University, Ithaca, New York 14850
(Received 29 June 1973)

Relativistic electron beams with $0.4 < \nu/\gamma < 2.2$ have been used in this experiment to heat a high-density $[n \sim (5-8) \times 10^{13}\ \mathrm{cm}^{-3}]$ fully ionized hydrogen plasma immersed in a magnetic field. The resulting heating levels are strongly dependent on the effective diode impedance $Z = V/I$ and, correspondingly, the ν/γ of the beam. Measurements of the total plasma energy from the plasma diamagnetism and the ion energy distribution from analyses of charge-exchange neutral atoms are used to determine scaling laws for the beam-plasma interaction.

Recent experiments[1-5] using high-energy relativistic electron beams have demonstrated the transfer of electrical energy into plasma thermal energy. The heating mechanism involves collective beam-plasma interactions, with two candidates being most likely: turbulent heating resulting from the beam return current[6-8] ($\nu/\gamma > 1$), and two-stream instabilities[8,9] with $\nu/\gamma \sim 1$.

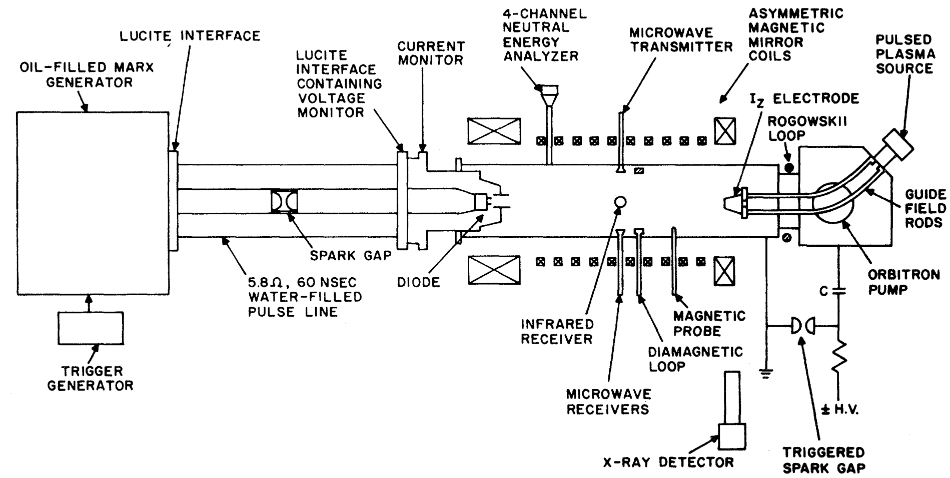

FIG. 1. Schematic of experiment.

The Cornell University turbulent-heating experiment[10,11] has been modified (Fig. 1) to allow the introduction of a relativistic electron beam from a 5.8-Ω Pocobeam[12] accelerator capable of operating at ≤ 500 kV with ≤ 86 kA currents for a nominal 60-nsec pulse. A nonsymmetric magnetic mirror field (~ 150 cm axial length) is energized by a 120-kJ capacitor bank producing ~ 5–6 kG at one mirror, ~ 2.7 kG in the mirror well, and ~ 5 kG at the plasma-injection end. A set of hexapole-guide-field rods conducts plasma from a pulsed hydrogen plasma source through the (~ 5 kG) mirror peak into the trap. Plasma density has been measured with a 74-GHz fringe-shift interferometer and by the attenuation of a neutral atom beam where the microwaves are cut off.[10] The neutral background pressure is generally less than 4×10^{-6} T except when charge-exchange neutral-energy analysis is performed $P < 2\times10^{-5}$ T. The low background neutral pressure and the absence of plasma contact with the vacuum vessel are major differences between this experiment and previous efforts.[1-5]

In these experiments a foilless diode, positioned behind the peak of the mirror field, consisting of a carbon cathode and a cylindrical anode has been used to obtain impedances as low as 6 Ω. This diode relies on the leakage of low-density plasma from the mirror into the anode-cathode region to lower the effective diode impedance and guide the beam into the mirror. Anode structures with apertures of 2.5 and 5 cm have been used with appropriate carbon cathodes in this configuration.

Figure 2 indicates typical voltage, current, and plasma diamagnetism signals for electron beam heating. The presence of the injected fully ionized plasma in the diode region provides a stable impedance level with no evidence of diode closure for reasonable gap spacings ~ 1 cm. The diamagnetic signals displayed indicate the different time histories typical of various total energy levels within the mirror. For diamagnetic signals less than 35 J there was generally a slow decay characterized by a single time constant. Between 35 and 60 J, small discontinuities in the diamagnetic signal appeared. These were observed at various times following the rise of the

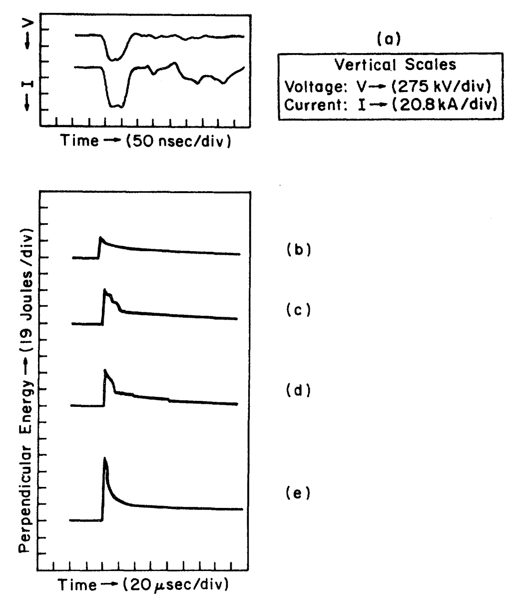

FIG. 2. Oscilloscope traces for (a) diode voltage and current, (b) plasma diamagnetism, $E_\perp < 35$ J, (c), (d) plasma diamagnetism, $E_\perp \sim 35$–60 J, and (e) plasma diamagnetism, $E_\perp > 60$ J.

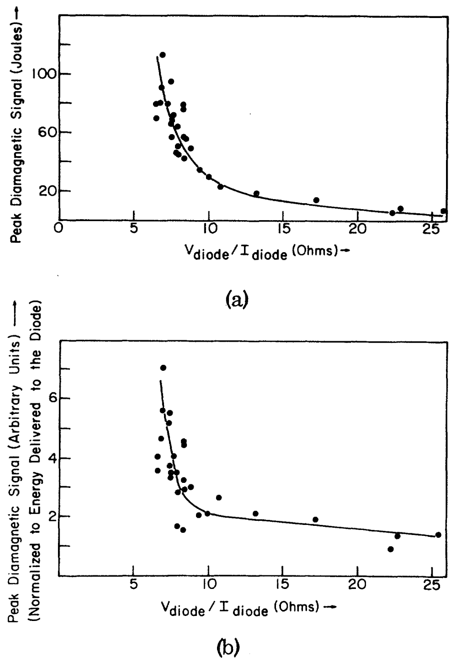

FIG. 3. (a) Peak plasma diamagnetism and (b) relative transfer efficiency for relativistic-electron beam heating using a 5-cm-aperture foilless diode. Each point corresponds to one machine firing. Peak transfer efficiencies from input energy into the diode to perpendicular plasma energy ~10–15%.

signal, from a few microseconds to over 100 μsec. They are attributed to sudden loss of energetic electrons through an instability, and are usually associated with bursts of hard x rays from the plasma. Finally, at the highest heating levels observed (60–100 J), the diamagnetic signal typically shows a rapid decay from its peak value followed by a transition to a much slower decay. This is interpreted as preferential electron heating at these levels, a view supported by charge-exchange neutral data discussed below. The microwave interferometer does not indicate any significant increase in density during the first few microseconds following heating. On a longer time scale (10–200 μsec) the plasma density increases substantially as cold plasma, and neutral gas from the plasma source enters the mirror region and is heated or ionized by impact with the confined hot plasma. Experiments[13] with a foiled diode at low currents determined a threshold for heating occurring at ~8–10 kA of diode current. This is nominally the level at which direct turbulent heating of the plasma occurs, suggesting that the same instabilities may be responsible for both types of heating at this level.

Figure 3 indicates the peak diamagnetic energy and the relative transfer efficiency measured for various diode impedance levels using a 5-cm foilless diode. These data were generated by adjusting both the beam firing time and the voltage level of the Marx generator since diode impedance is a very sensitive function of the timing between the plasma injection and beam firing. It is clear that for this type of direct beam-plasma interaction a low-impedance (high ν/γ) beam provided the highest energy transfer in the experiments reported.

In a separate experiment the mirror field peak at the electron beam diode was removed so that the field was increasing axially the entire length of the plasma column from the diode to the peak of the opposite mirror. Diamagnetic signals (nominally ~30 J) had a characteristic lifetime of ~1.5–2 μsec corresponding to plasma diffusion out one end of the machine as compared to traces in Fig. 2. The diamagnetic loop is electrostatically shielded with a metal foil and has a response time of ~$\frac{1}{2}$ μsec. This is taken as evidence that the diamagnetic signals are not due to trapped-beam primary electrons as the characteristic decay time without a mirror would be much shorter than the observed times.

Observation of the radial profile of the electron beam by insertion of slender 0.3–0.6-cm damage rods indicated that the beam was contained in the ~4 cm diam of the injected plasma column ~30 cm from the diode. At this axial position the magnetic field had decreased from ~5.5 kG at the mirror peak to ~3.6 kG. Possible fluting at the periphery of the beam was noted. At an axial position of ~67 cm (~2.7 kG) from the diode the beam usually had either disappeared or produced a diffuse weak damage pattern (5–10 cm). The use of even thin damage rods obstructed the flow of plasma into the diode region, changed the diode impedance and, consequently, the experimental conditions. This precluded the use of Faraday cups or calorimetry to determine beam parameters. Such behavior suggests that the beam is guided into the mirror by the injected plasma column which provides magnetic and electric neutralization for the beam. When one mirror was removed, as discussed previously, damage rods indicated that although the beam was weakened considerably it did not blow up.

Figure 4(a) shows the plasma diamagnetic energy contained in the mirror following the beam heating for various diode currents during a single run. For this configuration our plasma den-

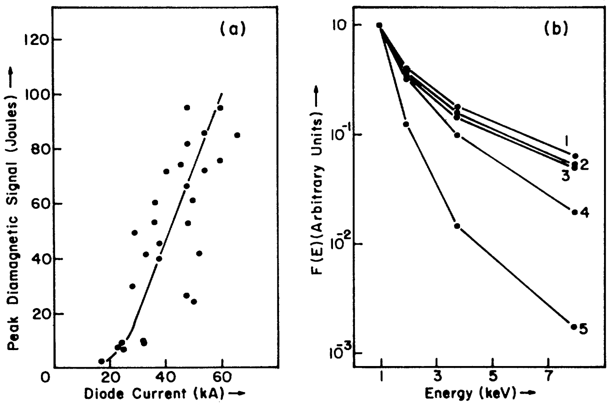

FIG. 4. (a) Perpendicular plasma energy versus diode current for a fixed beam-plasma injection time, i.e., ~constant impedance diode using a 2.5-cm-aperture foileless diode. (b) Ion distribution function versus energy for various beam heating levels. Curves 1–5, $E_\perp$=82, 74, 40, 30, 13 J, respectively, 1–4 with a 2.5-cm foilless diode and 5 using a 5-cm foiled diode.

sity per unit axial length $N \sim (1.5–2)\times10^{14}$ cm^{-1} corresponds to a mean perpendicular energy per electron-ion pair $\gtrsim$ 5 keV for 30 J in the mirror. To obtain these data the firing time of the electron beam relative to the time of plasma injection was held constant and the energy in the beam varied by charging the accelerator to different voltages. Each point corresponds to one machine firing. Data of the type displayed in Figs. 3 and 4(a) were obtained for both 2.5- and 5-cm foilless diodes, and data obtained with anode foils at low currents ($\leqslant$ 25 kA) are entirely compatible. In Fig. 3 beam voltages were in the range 250–500 kV, corresponding to a maximum Alfvén current of ~28.5 kA. It is evident that this is the approximate threshold region for strong beam heating which in this experiment corresponds to the condition $\nu/\gamma > 1$.

Figure 4(b) presents data acquired using a four-channel neutral-energy analyzer ~42 cm from the diode. Each curve corresponds to the data from one machine firing, and the curves labeled 1–4 are representative shots from Fig. 4. Curve 5 is shown for comparison to indicate appropriate scaling of the ion energy spectrum at low diamagnetic energies. These data were normalized at 925 eV because the absolute number of neutral atoms resulting from charge exchange is a sensitive function of the neutral krypton pressure, plasma density, energy, and expansion velocity, and therefore only relative levels are important.[10]

An examination of the ion distribution indicates that at low energies ($E_\perp \lesssim 40$ J $\approx$ 8 keV) changes in diamagnetic signal result in large changes in the ion distribution, while above this level the relative changes in the ion spectrum are a slower function of $E_\perp$. This may be indicative of preferential electron heating above average energies of ~8 keV or may result from the loss of confinement of ions during the heating process because of the low magnetic field ~3 kG at axial positions in front of the analyzer. Neutral data taken at an axial position ~120 cm from the diode in a region well past the axial extent of the electron beam indicated slowly rising neutral signals. This results from ion heating occurring near the diode region with subsequent diffusion of hot plasma into the aperture of the analyzer followed by charge exchange. This is consistent with observations of electron beam behavior with damage rods.

From the experimental results one concludes that relativistic electron beams can be used to heat fully ionized plasmas to energy densities of interest for controlled fusion. These plasmas appear to be stably confined immediately following heating, and it is possible to reliably transfer 10–15% of the electrical energy supplied to the diode into plasma perpendicular energy. In order to ensure maximum energy transfer it is necessary to have a sufficiently large magnetic field to suppress beam destruction via instabilities. Electron beams with $\nu/\gamma > 1$ appear to be most desirable for efficient plasma heating suggesting that the return current driven instabilities may be the most promising for plasma heating as predicted by Lovelace and Sudan.[6]

The authors wish to thank Professor N. Rostoker and Professor R. Sudan for many valuable discussions, and Dr. S. H. Robertson and Mr. M. A. Greenspan for assistance with the neutral-atom energy analyzer.

---

*Research supported in part by the U. S. Atomic Energy Commission and the Office of Naval Research.

[1]A. T. Altyntsev *et al.*, Pis'ma Zh. Eksp. Teor. Fiz. 13, 197 (1971) [JETP Lett. 13, 139 (1971)], and in *Proceedings of the Fourth International Conference on Plasma Physics and Controlled Nuclear Fusion Research, Madison, Wisconsin, 1971* (International Atomic Energy Agency, Vienna, 1972), Vol. 2, p. 309.

[2]C. A. Kapetanakos and D. S. Hammer, Appl. Phys. Lett. 23, 17 (1973); C. A. Kapetanakos *et al.*, Bull. Amer. Phys. Soc. 17, 1032 (1972).

[3]P. A. Miller and G. W. Kuswa, Phys. Rev. Lett. 30, 958 (1973).

[4]G. C. Goldenbaum *et al.*, Bull. Amer. Phys. Soc. 17, 1031 (1972).
[5]C. Stallings *et al.*, Bull. Amer. Phys. Soc. 17, 1031 (1972).
[6]R. V. Lovelace and R. N. Sudan, Phys. Rev. Lett. 27, 1256 (1971).
[7]J. Guillory and G. Benford, Plasma Phys. 14, 1131 (1972).
[8]A. A. Ivanov and L. I. Rudakov, Zh. Eksp. Teor. Fiz. 58, 1332 (1970) [Sov. Phys. JETP 31, 715 (1970)].
[9]L. E. Thode and R. N. Sudan, Phys. Rev. Lett. 30, 732 (1973).
[10]S. Robertson, P. Korn, and C. B. Wharton, IEEE Trans. Plasma Sci. 2, 17 (1973).
[11]C. Wharton *et al.*, in *Proceedings of the Fourth International Conference on Plasma Physics and Controlled Nuclear Fusion Research, Madison, Wisconsin, 1971* (International Atomic Energy Agency, Vienna, 1972), Vol. 2, p. 25.
[12]Manufactured by Maxwell Laboratories, Inc.
[13]P. Korn, F. Sandel, and C. B. Wharton, in Proceedings of the Sixth European Conference on Controlled Fusion and Plasma Physics, Moscow, U.S.S.R., 30 July–3 August 1973 (to be published).

Shear Viscosity and Ultrasonic Absorption near a Plait Point in the Ternary System Water-Benzene–Ethyl Alcohol

Laura Guidoni and Vincenza Viti
Laboratori di Fisica, Istituto Superiore di Sanità, Roma, Italia

and

G. D'Arrigo, L. Mistura, and P. Tartaglia
Facoltà di Ingegneria, Istituto di Fisica, Università di Roma, Roma, Italia, and Gruppo Nazionale di Struttura della Materia del Consiglio Nazionale delle Ricerche, Roma, Italia
(Received 31 May 1973)

The kinematic shear viscosity and the ultrasonic absorption coefficient have been measured in the ternary system water-benzene–ethyl alcohol near a critical point ("plait point") (P_c=1 atm; T_c=25°C; critical composition in wt%: water, 10.25; benzene, 52.10; and ethyl alcohol, 37.25), to provide a qualitative test of recent theoretical predictions. The experimental results indicate a rapid increase of the shear viscosity as a function of concentration near the plait point and a less pronounced sensibility of the absorption coefficient.

Recent theoretical works[1-3] have renewed the interest in the experimental study of critical phenomena in multicomponent systems. These works are primarily concerned with equilibrium properties. A few theoretical predictions concerning the critical behavior of dynamical properties in fluid mixtures have been made.[4-6] According to these predictions we expect shear viscosity to exhibit always the same anomaly irrespective of the number of components and the type of critical point, while ultrasonic absorption should be less and less affected by critical fluctuations as the number of components increases. The purpose of the present Letter is to report on recent experiments which have been made to provide a qualitative test of these theoretical predictions. Both kinematic viscosity η/ρ and ultrasonic absorption coefficient α have been measured as a function of temperature and concentration in the one-phase homogeneous region of the liquid system water-benzene–ethyl alcohol (WBE) near a plait point.

From the historical point of view it may be of interest to report that an anomalous behavior of shear viscosity near a plait point of the ternary system water-benzene–acetic acid was first observed by Friedländer[7] in 1901. His results were later (1946) confirmed by an extensive work on twelve ternary systems by Mondain-Monval and Quiquerez.[8] On the other hand, to our knowledge ours are the first reported measurements on the behavior of sound absorption near a critical point in ternary systems.

The mixture WBE belongs to that type of ternary system in which the mixing of the three components leads to the formation of one pair of liquid layers in equilibrium, each one containing a proper amount of every component. Water and benzene are partially miscible but each can dissolve in all proportions in ethyl alcohol. Therefore, if we gradually add alcohol to an appropriate heterogeneous water-benzene mixture, the